Refereed Proceedings

The 13th International Conference on Fluidization - New Paradigm in Fluidization Engineering

Engineering Conferences International *Year* 2010

DIRECT NUMERICAL SIMULATION OF FLUIDIZED BED WITH IMMERSED BOUNDARY METHOD

Kenya Kuwagi* H. Utsunomiya† Y. Shimoyama‡
H. Hirano** T. Takami††

*Okayama University of Science, kuwagi@mech.ous.ac.jp
†Okayama University of Science
‡Okayama University of Science
**Okayama University of Science
††Okayama University of Science

Direct Numerical Simulation of Fluidized Bed with Immersed Boundary Method

Kuwagi K.[a], Utsunomiya H.[a], Shimoyama Y.[a], Hirano H. [b] and Takami T.[a]
[a] Dept. of Mech. Eng., Okayama University of Science, Okayama 700-0005, Japan
[b] Dept. of Applied Chem. and Biotech., Okayama University of Science, Okayama 700-0005, Japan

ABSTRACT

The applicability of the immersed boundary (IB) method, which is one of direct numerical simulations (DNS) for multiphase flow analyses, has been examined to simulate a fluidized bed. The volumetric-force type IB method developed by Kajishima et al. (2001) has been applied in the present work. While particle-fluid interaction force is calculated with the surface integral of fluid stress at the interface between particle and fluid in the standard IB method, the volume integral of interaction force is used in the volumetric-force type IB method. In order to validate the present simulation code, drag force and lift force firstly were calculated with IB method. Then calculated drag coefficients were compared with values estimated with Schiller-Nauman and Ergun equations, while calculated lift coefficients were compared with the previous simulated results. The difference of drag was within approximately 1% except in the range of low Reynolds number. Thus, the accuracy of the present simulation code was confirmed. Next, simulation of fluidized bed was carried out. Since DNS requires a large computer capacity, only 400 particles were used. The particle is 1.0mm in diameter and 2650kg/m^3 in density. From the simulated results, concentrated upward stream lines from the bottom wall were observed in some regions. This inhomogeneous flow would be attributed to particulate structure.

INTRODUCTION

The Discrete Element Method (DEM) and Computer Fluid Dynamics (CFD) coupling model recently has played a large role in fluidized bed research because it can incorporate the factors of the problems associated with agglomerate (1), sintering (2), attrition and/or erosion (3). Furthermore, its application spreads to circulating fluidized beds (CFBs) (4). Particle-fluid interaction, e.g. lift force and viscous torque, usually are not considered in a bubbling fluidized bed because a particle often collides/contacts with other particles and free path of a particle is short. On the other hand, the free path in a CFB is longer. Accordingly, the effect of lift force and viscous torque would be larger and can not be ignored. However, DEM can not directly capture a phenomenon whose scale is less than particle size, e.g. drag force, lift force and lubrication force around particles. Zhang et al. (5) examined the effect

of lubrication force on the particle collision and reported that it affects restitution coefficient in the spring-dashpot model of DEM. For such problems, Direct Numerical Simulation (DNS) would be effective. There are many DNS methods for the analyses of multiphase flow. Pan et al. (6) carried out the direct numerical simulation of fluidization with Finite Element Method. In their simulation, simulation mesh was constructed at each time step. Accordingly, this method requires large computer capacity. On the other hand, Kajishima et al. (7) developed the body force type IB method to analyze turbulent flow in gas-solid two-phase flow. Since the Cartesian coordinates is utilized in their method and the shape of simulation mesh is rectangular, the computer load is light and the programming is easy. Generally, DNS requires large computer capacity. Thus the above advantage is very attractive. Nishiura et al. (8) used the body force type IB method to simulate hindered settling behavior of particle.

In the present study, the applicability of the body force type IB method on the analyses of fluidized bed was examined. The accuracy firstly was checked from the analyses of lift forces (Saffman force and Magnus force) and viscous torque. Then the simulation of fluidized bed was carried out.

NUMERICAL CALCULATION

Immersed Boundary Method

The Immersed Boundary (IB) method, which is one of direct numerical simulations, was applied. The body force type IB method developed by Kajishima et al. (7) was utilized in this numerical calculation.
The governing equations are as follows:
<Gas phase>

$$\nabla \cdot u = 0 \tag{1}$$

$$\frac{D\vec{u}}{Dt} = -\frac{1}{\rho_g}\nabla p + \vec{f}_{vis} + \vec{f}_{ib} + \vec{g} \tag{2}$$

where $\vec{f}_{ib}$ is the body force term to force the velocity in a calculation cell where a particle occupies to be the particle velocity and expresses as follows:

$$\vec{f}_{ib} = \varepsilon_p(\vec{v}_p - \vec{u})/\Delta t \tag{3}$$

The particle volume fraction ε_p at interface cell was calculated with the method of Tsuji et al. (9).
<Particle phase>

$$\frac{d(m_p\vec{v}_p)}{dt} = \int_{S_p}\vec{\tau}\cdot\vec{n}dS + \vec{F}_{ext} = -\rho_g\int_{V_p}\vec{f}_{ib}dV + \vec{F}_{ext} \tag{4}$$

$$\frac{d(\vec{I}_p\cdot\vec{\omega}_p)}{dt} = \int_{S_p}\vec{r}\times(\vec{\tau}\cdot\vec{n})dS + \vec{T}_{ext} = -\rho_g\int_{V_p}\vec{r}\times\vec{f}_{ib}dV + \vec{T}_{ext} \tag{5}$$

Analysis conditions

A schematic of the system is shown in Fig.1. The fluid flow is injected from the bottom wall. The thickness of the domain basically was set to be equal to the particle diameter. However, the thickness was changed in some calculations to examine its effect. A particle was fixed at the center of the analysis domain in the case of calculations for drag force, lift force and viscous torque. The analysis conditions for drag force, lift force and viscous torque are shown in Table 1. The size of the analysis area and calulation mesh was changed to examine the accuracy of the present simulation under the conditions shown in Table 2. In addition, the analysis conditions for a fluidized bed are shown in Table 3.

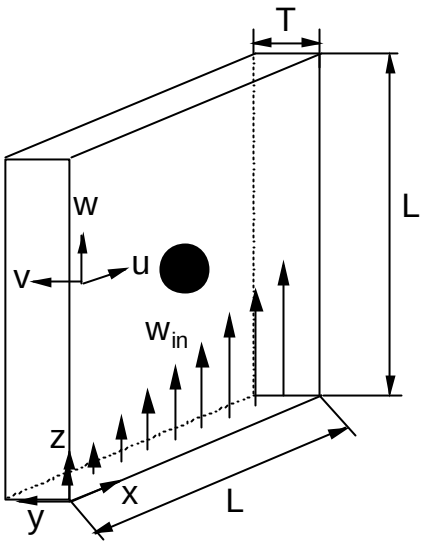

Fig. 1 Schematic of the system

The simulated results were examined in terms of lift coefficient and dimensionless torque which can be defined as follows:

$$C_L = F_L \Big/ \frac{1}{2}\rho_g u_c{}^2 A \tag{6}$$

$$C_{LR} = F_{LR} \Big/ \frac{1}{2}\rho_g \frac{|\vec{u}_r|}{|\vec{\omega}_r|}\vec{u}_r \times \vec{\omega}_r A \tag{7}$$

$$C_T = \frac{1}{2} T_f \rho_g r^5 |\vec{\omega}_r| \vec{\omega}_r \tag{8}$$

Table 1 Calculation conditions

Case 1 (Drag force)	
Particle Reynolds number: Re_p	0.1, 0.5, 1.0, 5.0, 10.0, 50.0, 100.0, 500.0
Case 2 (Saffman lift force)	
Particle Reynolds number: Re_p	1.374, 3.434, 13.74, 68.68, 137.4, 274.4, 480.8
Velocity gradient: $a^* = (r_p / w)(\partial w / \partial x)$	0.1
Case 3 (Magnus lift force)	
Particle Reynolds number: Re_p	1.099, 5.495, 32.97, 65.93, 82.42, 109.9
Rotation Reynolds number: Re_R	0.137, 0.275, 0.412, 0.549, 0.687, 1.374
Case 4 (Viscous Torque)	
Rotation Reynolds number: Re_R	0.137, 0.275, 0.412, 0.549, 0.687, 1.374

Table 2 Calculation conditions for analysis area

Case Number	L/d_p	T/d_p	Δ/d_p
1-1	5	1	1/10
1-2	15	1	1/10
1-3	5	2	1/10
2-1	5	1	1/10
2-2	5	5	1/10
2-3	10	1	1/10
3-1	5	1	1/10
3-2	5	5	1/10
3-3	5	1	1/20
4-1	5	1	1/10
4-2	10	1	1/10
4-3	5	1	1/20

Δ: Simulation mesh size

Table 3 Conditions for fluidization simulation

Particle	
diameter: d_p [mm]	1.0
density: ρ_p [kg/m^3]	2650
number [#]	400
Gas	Air
density: ρ_g [kg/m^3]	1.15
viscosity: μ_g [Pa s]	1.75×10^{-5}
superficial velocity [m/s]	2.0
Column	
Width x Height x Thickness [mm]	30 x 30 x 1(=d_p)
Simulation time step [s]	1.0×10^{-6}

Numerical Procedure

Time discretization was approximated by an explicit method and the inertial terms by 3rd order up-wind scheme. The pressure distribution was solved with the HS-MAC (SOLA) method. The boundary conditions for drag force, lift force and viscous torque analyses are as follows:

$u = v = 0, \quad \frac{\partial w}{\partial x} = 0$ at x=0, L (w=0 for viscous torque analysis)

$\frac{\partial u}{\partial y} = \frac{\partial w}{\partial y} = 0, \quad v = 0$ at y=0, d_p

$u = v = 0, \quad w = w_{in}$ at z=0 (w=0 for viscous torque analysis)

$\frac{\partial u}{\partial z} = \frac{\partial v}{\partial z} = \frac{\partial w}{\partial z} = 0$ at z=L (u=v=w=0 for viscous torque analysis)

On the other hand, those for fluidized bed analysis are as follows:

$u = v = w = 0$ at x=0, L

$\frac{\partial u}{\partial y} = \frac{\partial w}{\partial y} = 0, \quad v = 0$ at y=0, d_p

$u = v = 0, \quad w = w_{in}$ at z=0

$\frac{\partial u}{\partial z} = \frac{\partial v}{\partial z} = \frac{\partial w}{\partial z} = 0$ at z=L

The simulations were carried out on a personal computer whose spec is presented in Table 3. Since the DNS generally requires large computer capacity, researchers often use a parallel supercomputer or other special computer. Additionally, the load of present simulation method on a computer is not large.

Table 3 Computer spec used in the present research

OS	Windows 7 Professional (64bit)
Processor	Intel (R) Core (TM) i7 CPU 920 @ 2.67GHz
Memory	12.0GB

RESULTS AND DISCUSSION

Lift forces and viscous torque

Figure 2 shows the drag coefficient. Kajishima et al. (7) reported that the difference between simulated and estimated values is 10 to 19% in the case of Δ/d_p=1/8 and 1 to 7% in the case of Δ/d_p=1/10. For the present results with Δ/d_p=1/10 (Case 1-1), the difference is 50% at low Reynolds number. This would be caused by the effect of the analysis area. Since the viscosity is dominant in the case of low Reynolds number, the effect of viscosity spreads widely. Accordingly, the analysis area would not be sufficient. Then the analysis area enlarged three times larger than previous one. As can be seen in the results of Case 1-2, the simulated values are smaller than estimated with Schiller-Nauman equation. Though the Schiller-Nauman equation is for a single particle, the present simulation with the thickness of particle's diameter corresponds to that particles line up in thickness direction, i.e. *y*-direction. When the thickness of the analysis domain is two times larger (Case 1-3), the simulated values are in good agreement with the estimated ones. The difference is 0.1 to1% except in the range of low Reynolds number.

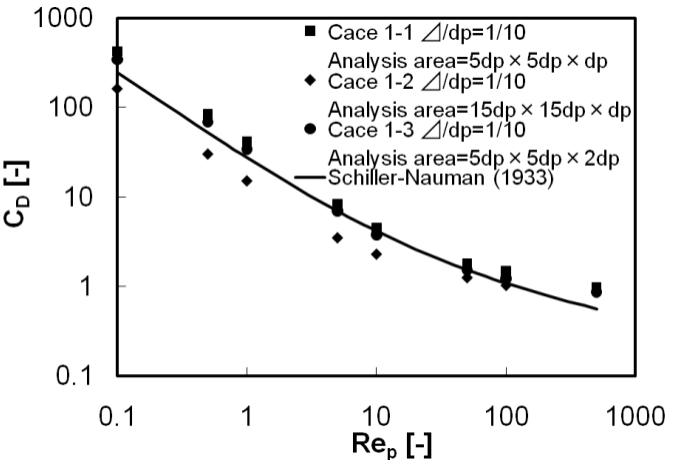

Fig. 2 Drag coefficient

Figure 3 shows the lift coefficient of Saffman force which is the lift force caused by the flow with velocity gradient around a particle. The simulated lift force of Case 2-1 is larger than the results of McLaughlin (10) at low Reynolds Number. On the other hand, the result with the two times larger thickness (Case 2-1) is larger than the

result of Case 2-1. To the contrary, the result with the two times wider analysis region is smaller and closer to that of McLaughlin (10). From these results, the effect of the analysis region is larger than that of the thickness.

Figure 4 shows the lift coefficient of Magnus force which the lift force is caused by rotational motion of particle. The rotating Reynolds number was set to 0.412 which corresponds to 30 rad/s of angular velocity. This value was obtained from DEM simulation in a fluidized bed (11). Though the simulated results in all cases well agreed with those of Oesterle and Dinh(12), the tendency is different at high Reynolds number.

Figure 5 shows the results of viscous torque. The simulated results qualitatively agreed with Takagi's analytical solutions (13). However, the simulated values are half of the analytical solutions. Comparing (Case 4-1) with (Case 4-2), it is confirmed that the analysis area is not significant under the current conditions. On the other hand, the effect of the simulation mesh size is larger from the result of (Case 4-3). If the viscous torque is calculated more accurately, e.g. for the analysis of liquid fluidized bed, then the simulation mesh is required to be much finer.

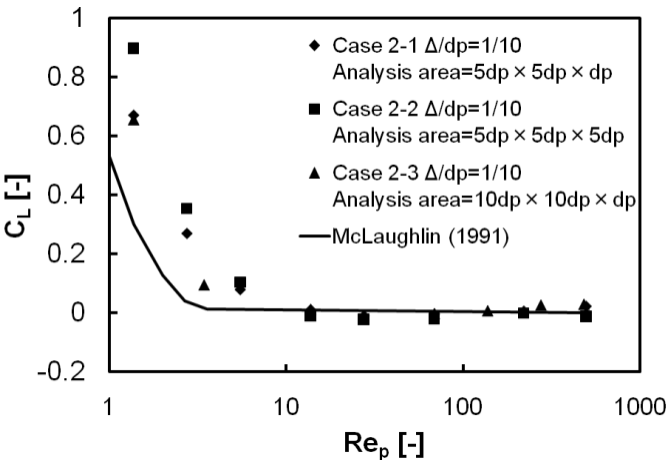

Fig. 3 Lift coefficient with a*=0.1

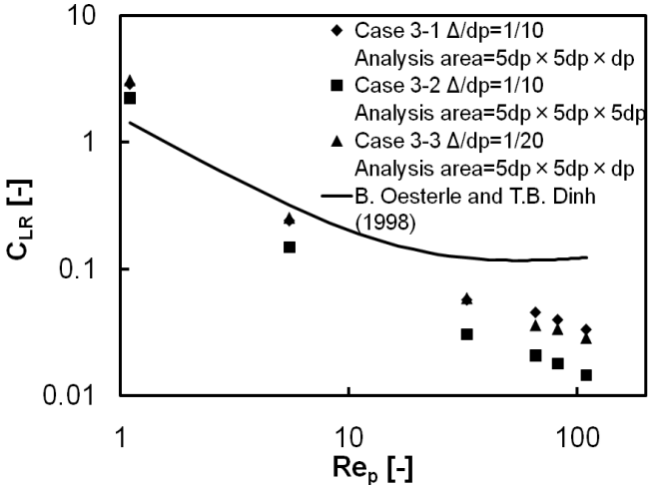

Fig. 4 Lift coefficient due to rotation at Re_R=0.412

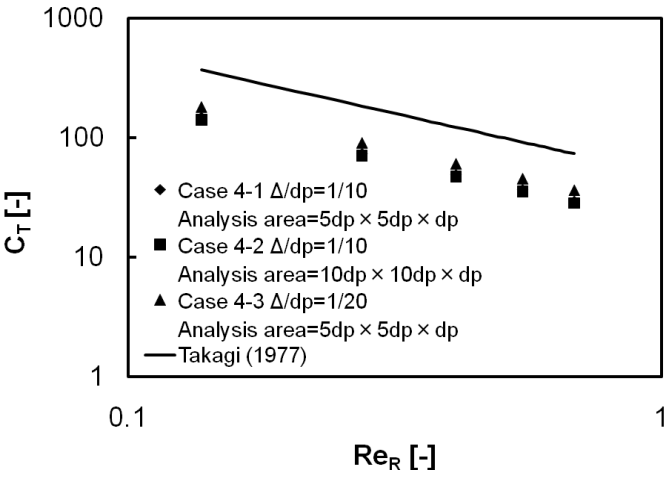

Fig. 5 Dimensionless torque at Re_p=0

Simulation of fluidized bed

Figure 6 shows the snapshot of fluidization with 400 particles. Complicate flow can be seen above the particles. Figure 7 shows the stream lines from the bottom wall drawn with an instantaneous velocity field data. Inhomogeneous flow can be observed inside the bed. There are some regions where lines are concentrated. This would bed caused by particulate structure.

Measured minimum fluidizing velocity was 1.5m/s. This value is much larger than the one estimated with Wen-Yu equation. Since the bed size is small, the effect of wall friction would become larger. Thus this would be caused by relatively large wall friction. For this simulation, it took about 3 weeks to simulate the real 1.0 second.

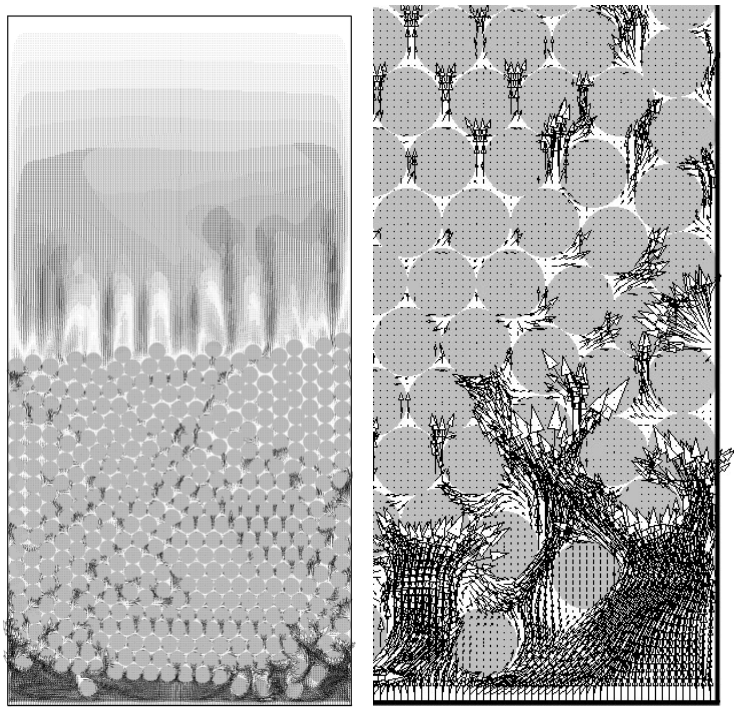

(a) (b)

Fig. 6 Snapshot of fluidization
(a) whole region
(b) Magnification of lower right area of Fig.(a)

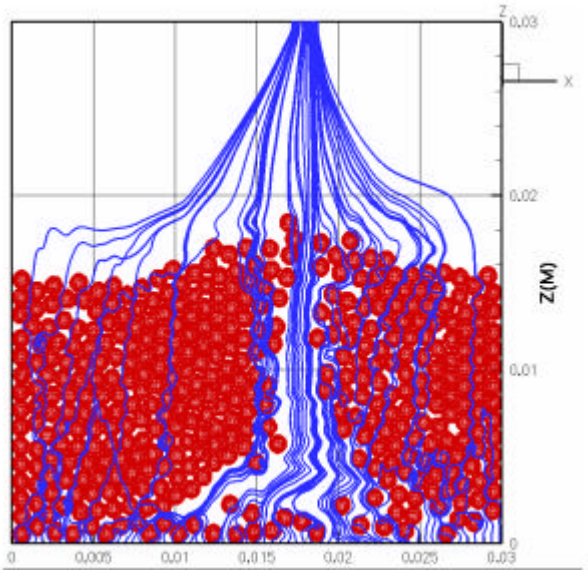

Fig. 7 Stream lines from the bottom wall

CONCLUSIONS

In order to examine the applicability of the volumetric-force type immersed boundary (IB) method to the simulation of fluidized bed, drag force, lift force and viscous torque were calculated. When the simulation mesh size is 1/20 of the particle diameter, the drag force and lift force were calculated with high accuracy. On the other hand, mach finer mesh size is needed for the calculation of viscous torque.

Then a simulation of fluidization was carried out. Inhomogeneous gas flow was observed in the particle bed. All simulations successfully were carried out with a personal computer because of a

relatively light load on a computer with the volumetric-force type IB method. However, the problem in simulation run time with a personal computer still remains.

ACKNOWLEDGEMENT

This work was supported by the Ministry of Education, Cultural, Sports, Science and Technology of Japan through a Financial Assistance Program of the Social Cooperation Study (2006-2010).

NOTATION

A	projected area ($=\pi r_p^2$) (m^2)
a^*	dimensionless velocity gradient (-)
C_L	lift coefficient (-)
C_{LR}	lift coefficient due to rotation (-)
C_T	dimensionless torque (-)
d_p	particle diameter (m)
F_{ext}	external force (N)
f_{ib}	body force in IB method (N/m^3)
f_{vis}	viscous force (N/m^3)
g	gravitational acceleration (m/s^2)
I_P	inertia moment of particle (kgm^2)
L	width and height of analysis domain (m)
m_p	particle mass (kg)
P	pressure (Pa)
Re_p	particle Reynolds number (m)
Re_R	rotating Reynolds number (-)
r_p	particle radius (m)
T	thicness of analysis domain (m)
T_{ext}	external moment (Nm)
T_f	viscous torque (Nm)
t	time (s)
u	gas velocity in x-direction (m/s)
u_r	relative velocity (m/s)
v	gas velocity in y-direction (m/s)
v_P	particle velocity (m/s)
w	gas velocity in z-direction (m/s)
x, y, z	coordinate (m)

Greek letters

Δ	simulation mesh size (m)
μ_g	gas viscosity (Pa s)
ρ_g	gas density (kg/m^3)
ρ_p	paritcle density (kg/m^3)
ε_p	particle volume fraction (-)
ω_p	angular velocity of particle (rad/s)

REFERENCES

(1) Mikami, T., Kamiya, H. and Horio, M., *Chem. Eng. Sci.*, 53-10 (1998), 1927-1940.
(2) Kuwagi, K., Mikami, T. and Horio, M., *Powder Technol.*, 109 (2000), 27-40.
(3) Rong, D. and Horio, M., *Int. J. Multiphase Flow*, 27 (2001), 89-105.
(4) Chu, K.W., Wang, B. and Yu, A.B., *Fluidization XII*, (1998), 735-742.
(5) Zhang, W., Noda, R. and Horio, M., *Powder Technol.*, 158 (2005), 92-101.
(6) Pan, T. W., Joseph, D. D., Glowinski, R, Bai, R. and Sarin, V., *J. Fluid Mech.*, 451 (2002), 169-191.
(7) Kajishima, T., Takiguchi, S., Hamasaki, H. and Miyake, Y., *JSME Int. Journal B*, 44-4, (2001) pp. 526-535.
(8) Nishimura, D., Shimosaka, A., Shirakawa, Y. and Hidaka, J., *Kagaku Kogaku Ronbunshu*, 32-4 (2006) pp. 331-340
(9) Tsuji, T., Narutomi, R. Yokomine, T., Ebara, S. and Shimizu, A., *Int. J. Multiphase Flow*, 29, (2003) pp. 1431-1450.
(10) McLaughlin, J.B., *J. Fluid Mech.*, 224, (1991) pp.261-274.
(11) Kuwagi, K., Takano, K. and Horio, M., *Powder Technology*, 113, (2000) pp.287-198.
(12) Oesterle, B. and Dinh, T.B., *Experiments in Fluids*, 25, (1998) pp.16-22.
(13) Takagi, H, *J. Phys. Soc. Japan*, 42-1, (1977) pp. 319-325.